Numerical Investigation on Initiation Process of Spherical Detonation by Direct Initiation with Various Ignition Energy

Takayuki Nirasawa, and Akiko Matsuo
Keio University, 3-14-1, Hiyoshi, Kohoku-ku, Yokohama, Kanagawa, 223-8522, Japan
mr061857@hc.cc.keio.ac.jp

Keywords: Direct Initiation, Spherical Detonation, Ignition Energy, CFD

Abstract

In order to investigate the initiation and propagation processes of a spherical detonation wave induced by direct initiation, numerical simulations were carried out using two-dimensional compressible Euler equations with an axisymmetric assumption and a one-step reaction model based on Arrhenius kinetics with various levels of ignition energy. By varying the amount of ignition energy, three typical initiation behaviors, which were subcritical, supercritical and critical regimes, were observed. Then, the ignition energy of more than 137.5×10^6 in non-dimensional value was required for initiating a spherical detonation wave, and the minimum ignition energy (i.e., critical energy) was less than that of the one-dimensional simulation reported by a previous numerical work.

When the ignition energy was less than the critical energy, the blast wave generated from an ignition source continued to attenuate due to the separation of the blast wave and a reaction front. Therefore, detonation was not initiated in the subcrtical regime. When the ignition energy was more than the minimum initiation energy, the blast wave developed into a multiheaded detonation wave propagating spherically at CJ velocity, and then a cellular pattern radiated regularly out from the ignition center in the supercritical regime. The influence on ignition energy was observed in the cell width near the ignition center, but the cell width on the fully developed detonation remained constant during the expanding of detonation wave due to the consecutive formation of new triple points, regardless of ignition energy. When the ignition energy was equal to the critical energy, the decoupling of the blast wave and a reaction front appeared, as occurred in the subcrtical regime. After that, the detonation bubble induced by the local explosion behind the blast wave expanded and developed into the multiheaded detonation wave in the critical regime. Although few triple points were observed in the vicinity of the ignition core, the regularly located cellular pattern was generated after the onset of the multiheaded detonation. Then, the average cell width on the fully developed detonation was almost to that in the supercritical regime. These numerical results qualitatively agreed with previous experimental works regarding the initiation and propagation processes.

Introduction

Detonation is a supersonic combustion wave propagating with a leading shock wave. Previous investigations have clarified that detonation has an unsteady and complicated structure with a transverse wave propagating lengthwise and crosswise, and that the trajectory of triple points at the intersecting lines of triple shock waves records a cellular pattern on smoked- foil.

In generally, there exist two methods to initiate detonation wave [1]. One method is referred to as DDT (Deflagration-to-Detonation Transition), in which detonation is initiated by flame acceleration from subsonic speed to supersonic. Then, turbulence effect and the interaction between compression waves and flame play the important role for initiating detonation. The other method is referred to as direct initiation, in which a high-energy core induces a strong blast wave to trigger detonation, and an ignition source plays a dominant role for the detonation initiation. In this study, detonation is initiated by direct initiation.

Previous studies on direct initiation have reported that there exists a minimum energy for initiating detonation, and the initiation behaviors are categorized into three regimes (i.e., subcritical, supercritical, and critical regimes), according to ignition energy [1-9]. When the ignition energy is below the minimum initiation energy (subcritical regime), a reaction front is decoupled from the blast wave generated from a high-energy core just after ignition. Subsequently, the blast wave attenuates during propagation and becomes a sound wave, and detonation is not initiated. When the ignition energy is above the initiation energy (supercritical regime), the blast wave directly develops into a multiheaded detonation wave in the CJ (Chapman-Jouguet) state. The cell rapidly grows near the ignition source, and the growth rate is determined by the amount of ignition energy [4]. When the ignition energy is at the minimum initiation energy (critical regime), the decoupling of a blast wave and a reaction front is observed, as occurs in the subcritical regime. After that, the blast wave and the reaction front propagate at constant velocity, during what is called the quasi-steady period. When the quasi-steady state terminates, the detonation bubble induced by the local explosion behind the blast wave develops into an asymmetric detonation wave with transverse waves, and this process is referred to as detonation reestablishment [1, 6]. Lee and Ramamurthi have proposed Detonation Kernel [2] in order to formulate critical energy value. It is based on the concept that detonation is initiated

when a blast wave decay to critical condition, where the influence of chemical reaction is as large as that of ignition source at critical radius. They have suggested pressure and Mach number in the half-CJ state as the critical condition.

The experimental study on cylindrical detonation by Vasil'ev and Trotsyuk [7] has demonstrated that there are two stages in the expanding of the detonation front in the critical regime. In the first stage, which is observed near the ignition source, the number of transverse waves decreases and cell width becomes larger due to attenuation of the detonation wave during propagation. In the second stage, the consecutive formation of new transverse waves appears in the course of the expanding of the detonation front.

In the numerical investigation on direct initiation by Mazaheri and Lee [6, 8], an artificial disturbance is set at a leading shock front in order to clarify the effect of a hot spot in the initiation of one-dimensional planar detonation. The result has demonstrated that the hot spot supports the decreases in minimum initiation energy and run-up distance. The numerical study by Eckett *et al*. [9] has demonstrated that the unsteadiness of induction zone is the most dominant factor in the failure of one-dimensional spherical detonation, as shown by numerical comparison of the effects of the unsteadiness, heat release, and curvature of flame. The two-dimensional numerical investigation on cylindrical detonation by Watt and Sharpe [10] has demonstrated that the cellular pattern strongly depends on grid resolution. As the resolution increases, the location where the triple points first appear gets closer to the ignition source and the cellular pattern becomes less regular. Additionally, new triple points are generated in the expanding of the detonation front. Authors have investigated the spherical detonation wave using two-dimensional compressible Euler equations for axisymmetry and a one-step reaction model [11]. Their simulation has reported that the results of two-dimensional analysis with circular grid system show good agreement with those obtained from one-dimensional simulation by Eckett *et al*. [9], regarding minimum initiation energy and detonation propagation. Meanwhile, the multi-dimensional wave structures such as transverse wave and triple points are observed in two-dimensional simulation with orthogonal grid system.

The objective of this study is to investigate the initiation and propagation processes of the spherical detonation induced by direct initiation with various levels of ignition energy using two-dimensional axisymmetric Euler equations. In addition, the cellular structure on the fully developed detonation is discussed.

Numerical Setup

Numerical target in this study is the spherical detonation wave induced by direct initiation. The system equations are two-dimensional compressible Euler equations with an axisymmetric assumption, and these are written as follows:

$$\frac{\partial \mathbf{Q}}{\partial t}+\frac{\partial \mathbf{E}}{\partial x}+\frac{\partial \mathbf{F}}{\partial y}=\mathbf{S}+\mathbf{H} \tag{1}$$

where $\boldsymbol{Q}$ is the conservative vector, and $\boldsymbol{E}$ and $\boldsymbol{F}$ are, respectively, the inviscid flux vectors in x and y directions. $\boldsymbol{S}$ and $\boldsymbol{H}$ are the source term vectors of chemical reaction and axisymmetry, respectively. These vectors are written by Eq. (2).

$$\mathbf{Q}=\begin{bmatrix}\rho\\ \rho u\\ \rho v\\ e\\ \rho Z\end{bmatrix}\quad \mathbf{E}=\begin{bmatrix}\rho u\\ p+\rho u^2\\ \rho uv\\ (e+p)u\\ \rho uZ\end{bmatrix}\quad \mathbf{F}=\begin{bmatrix}\rho v\\ \rho vu\\ \rho v^2+p\\ (e+p)v\\ \rho vZ\end{bmatrix}$$

$$\mathbf{S}=\begin{bmatrix}0\\ 0\\ 0\\ 0\\ \omega\end{bmatrix}\quad \mathbf{H}=-\frac{\rho v}{y}\begin{bmatrix}1\\ u\\ v\\ (e+p)/\rho\\ Z\end{bmatrix} \tag{2}$$

Here, ρ, u, v, p, e, Z and ω are density, x-velocity, y-velocity, pressure, total energy per unit volume, mass fraction of reactant and reaction rate of reactant, respectively. Reaction model in this study is a one-step irreversible chemical reaction model governed by Arrhenius kinetics. This simplified reaction model, in which only premixed gas is calculated under the assumption of calorically perfect gas without an actual induction length, is often used in detonation simulations [6, 8-11]. Total energy e and reaction rate ω are represented by Eqs. (3) and (4), respectively.

$$e=\frac{p}{\gamma-1}+\frac{\rho}{2}\left(u^2+v^2\right)+\rho QZ \tag{3}$$

$$\omega=-\rho KZ\exp(-E_a/T) \tag{4}$$

Where γ, E_a, K and Q are specific heat ratio, activation energy, frequency factor and exothermic heat release, respectively. These are chemical parameters in this reaction model. The values are identical to those in Ref. 9:

$$\begin{gathered}K/(\sqrt{RT_0}/L_{1/2})=70.8\\ E_a/RT_0=17.0\\ Q/RT_0=22.5\\ \gamma=1.2\end{gathered} \tag{5}$$

where R, T_0 and $L_{1/2}$ are gas constant, temperature ahead of a shock wave and half-reaction length, respectively. Half-reaction length is the distance

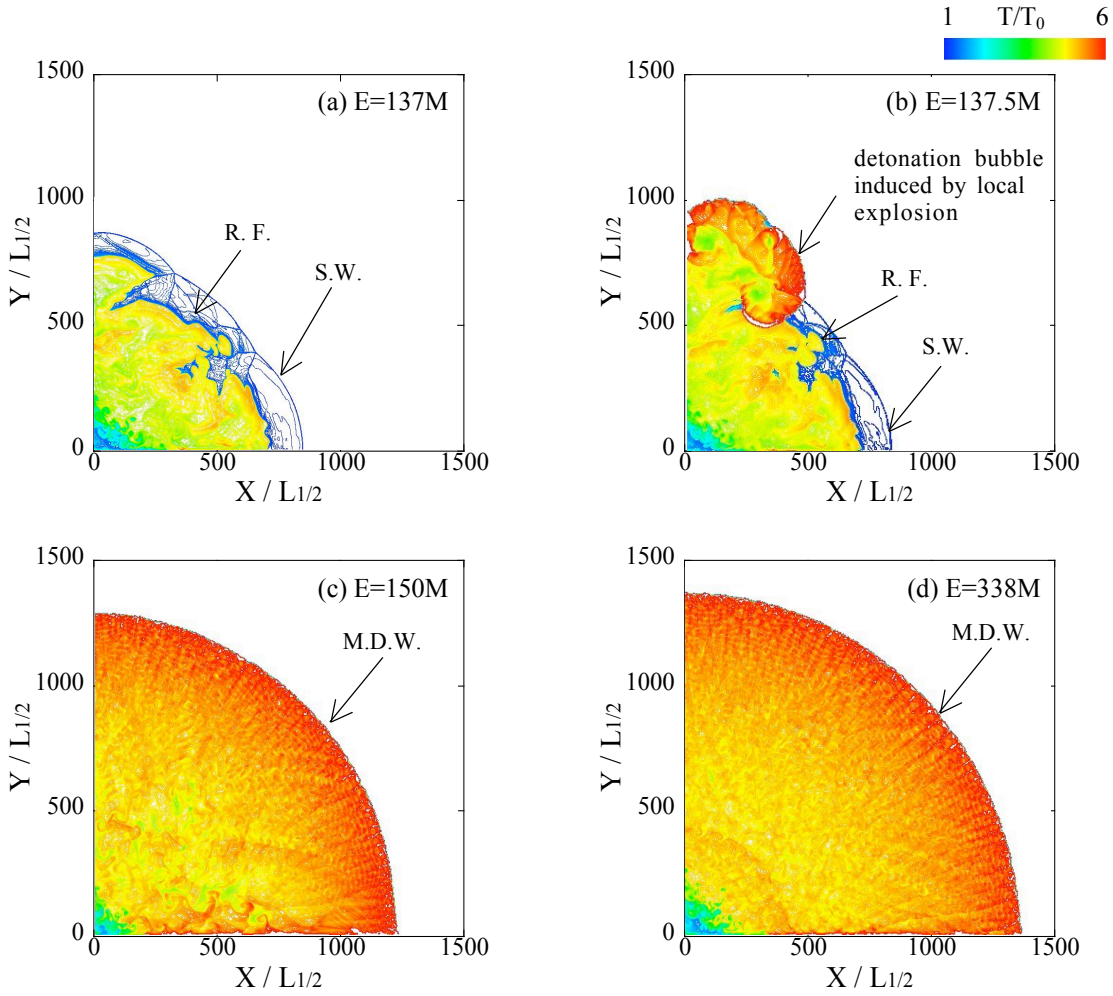

Fig. 1 Temperature distribution at t=300 for the ignition energy of (a) 137×10^6, (b) 137.5×10^6, (c) 150×10^6 and (d) 338×10^6. (S.W.: Shock Wave, R.F.: Reaction Front, M.D.W.: Multiheaded Detonation Wave)

required for mass fraction of reactant reducing to 0.5 in CJ detonation, and it is used as the unit length in this study. Grid resolution is defined by the number of grid points in half-reaction length, and 2 points per the length are set. As for the discretization method, the governing equations are integrated with an explicit second accuracy in time and in space scheme based on the non-MUSCL type TVD method [12], calculating source term point-implicitly.

The initial condition consists of two regions; one is the high-energy core of burned gas and the other is standard region of premixed gas. In the former region, the radius is fixed to $19L_{1/2}$ and the ignition energy normalized by standard pressure and half-reaction length E are changed from 100×10^6 to 338×10^6. Temperature and density are obtained from pressure and the equation for isentropic relation. According to the previous numerical study on one-dimensional detonation by Eckett *et al*. [9], spherical detonation is initiated when the ignition energy exceeds 166×10^6. The computational domain with uniform and orthogonal grid system is set at maximum of $2500L_{1/2}$, and there is no initial disturbance to create transverse waves. For the boundary condition, the mirror condition is used in the symmetric lines, and computational region expands during calculation in order to reduce computational load.

Results and Discussion

Ignition energy is changed in order to clarify the critical energy to initiate a spherical detonation wave in this calculation condition. Figure 1 shows the temperature distribution showing the detonation initiation or failure at t=300 for the ignition energy of (a) 137×10^6, (b) 137.5×10^6, (c) 150×10^6 and (d) 338×10^6. The result in the lowest energy case of Fig. 1a indicates the subcritical regime, in which the reaction front is decoupled from the leading shock wave and detonation is not initiated. In the subcritical regime, the leading shock wave continues to attenuate while propagation. Eventually, the blast wave becomes a sound wave, and the combustion terminates. In Fig. 1b, both the coupling and decoupling of the blast wave and the reaction front are observed. The detonation bubble generated by a local explosion expands, and the multi-dimensional structure is observed at the wave front. Subsequently, the detonation bubble develops into a multiheaded

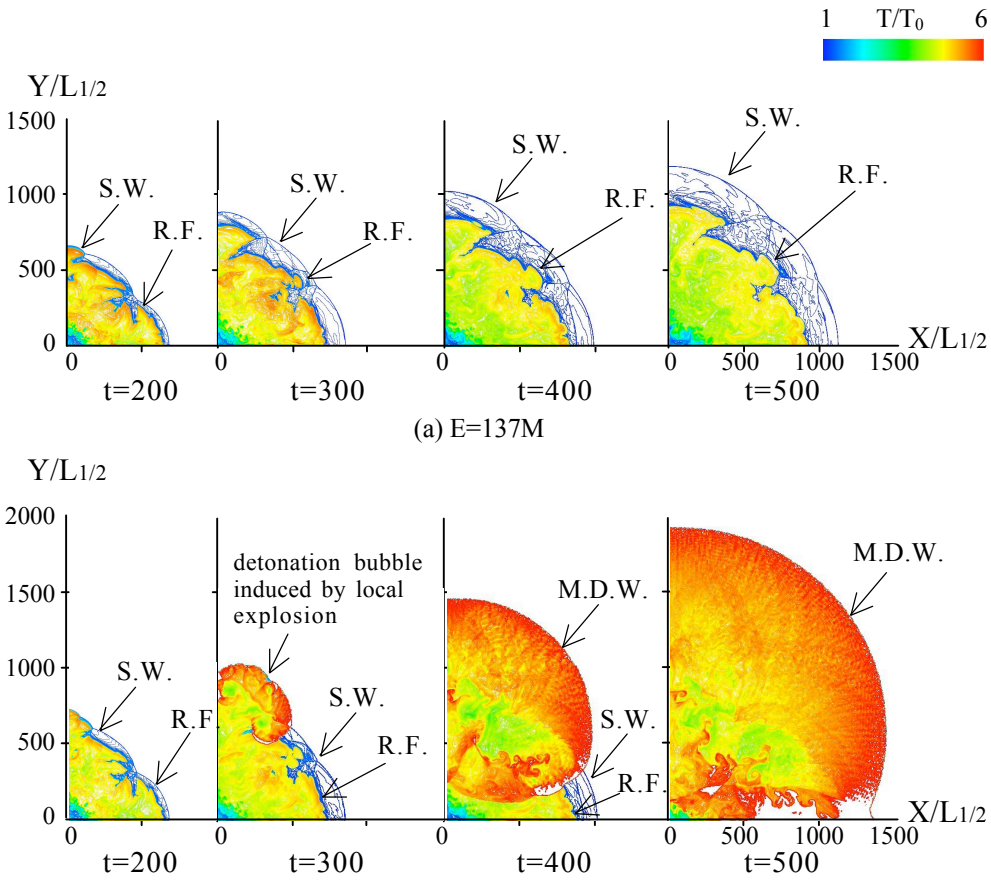

Fig. 2 Time evolution of temperature distribution at t=200, 300, 400 and 500 for the ignition energy of (a) 137×10^6 and (b) 137.5×10^6. (S.W.: Shock Wave, R.F.: Reaction Front, M.D.W.: Multiheaded Detonation Wave)

detonation wave. Therefore, this initiation process represents the critical regime. The result of Fig. 1c shows the fully developed spherical detonation wave in the supercritical regime. The detonation wave propagates spherically, and the wave structure of the expanding detonation is essentially the same as that of the detonation propagating in two-dimensional channel, which consists of transverse waves and triple points. In the highest energy case of Fig. 1d, the detonation expands spherically as well as the supercritical regime in Fig. 1c, resulting in the formation of a symmetric wave structure. The results in the supercritical regime of Figs. 1c and 1d imply that the wave structure on the fully developed detonation is independent of ignition energy. Under this chemical condition, the minimum ignition energy to initiate a spherical detonation wave directly in a two-dimensional axisymmetric system is 137.5×10^6, which is less than that of the one-dimensional spherical detonation by Ecketts' numerical study [9]. In addition, when the ignition energy is above 150×10^6, the detonation wave expands spherically with the transverse waves, referred to as the supercritical regime.

The initiation and failure processes near the critical energy are discussed using the time variation of flowfield. Figure 2 shows the time evolution of the propagation of a blast wave and a reaction front by temperature distribution in every time interval of 100 for the cases of (a) $E=137\times10^6$ and (b) $E=137.5\times10^6$. These conditions are the subcritical and critical regimes, respectively. At the lower energy of Fig. 2a, the reaction front is separated from the leading shock wave at t=200, and the distance between the blast wave and the reaction front spreads widely during the propagation. After t=300, the reaction front remains stationary, and the temperature at the reaction front becomes lower with the shock propagation. This means that the combustion hardly occurs, due to the increase of the induction time caused by attenuation of the blast wave. Eventually, a leading shock wave becomes to a sound wave, and combustion terminates. On the other hand, at the higher energy of Fig. 2b, the decoupling of the blast wave and the reaction front appears at t=200, as occurs in the subcritical regime of Fig. 2a. The detonation bubble induced by the local explosion expands as if the detonation bubble engulfs the blast wave, the shock-heated premixed gas and the reaction front at t=300 and t=400. Simultaneously, the detonation bubble develops into the multiheaded detonation wave during the propagation. As observed at t=400 in Fig. 2b, the mutiheaded detonation expands from the location where the local explosion occurs, resulting in the formation of an asymmetric

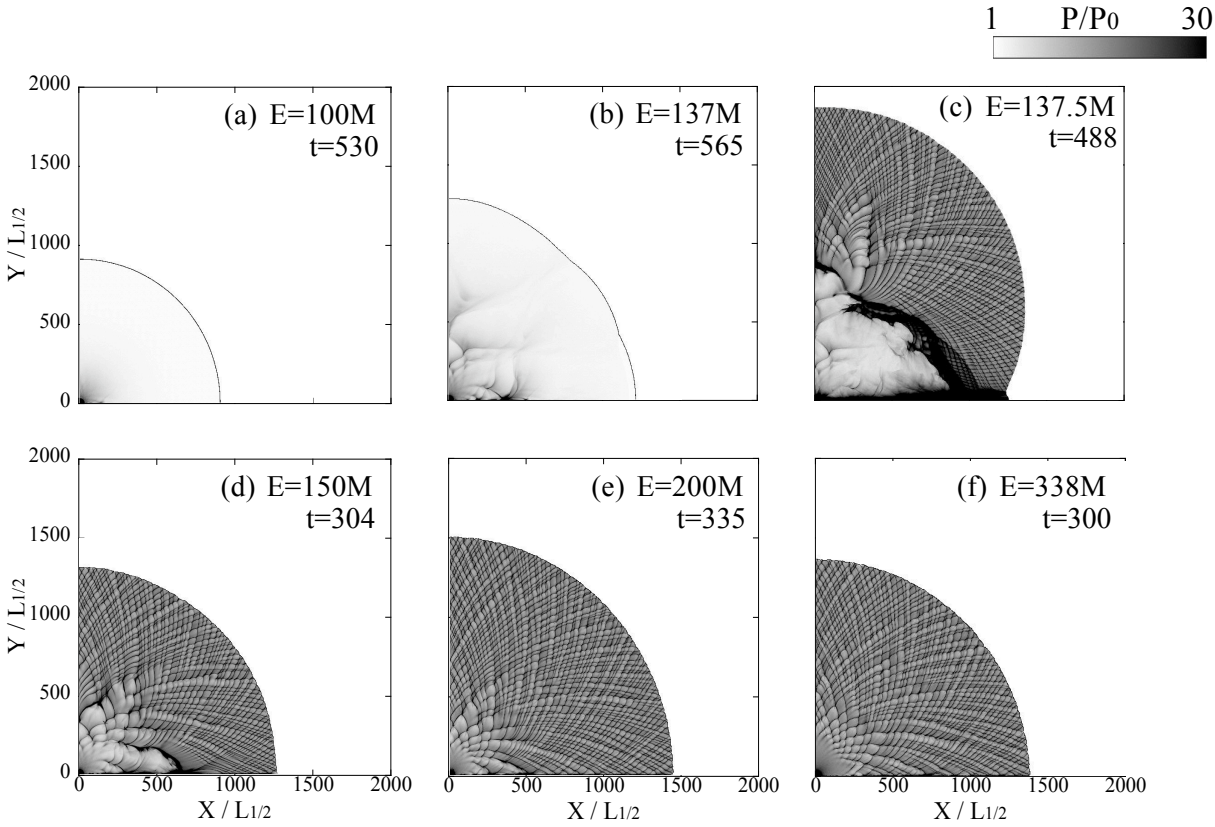

Fig. 3 Trajectory of triple points by maximum pressure contour at each time for the cases of (a) 100×10^6, (b) 137×10^6, (c) 137.5×10^6, (d) 150×10^6, (e) 200×10^6 and (f) 338×10^6.

structure. The initiation process caused by the local explosion is referred to as the detonation reestablishment, which is identical to the detonation initiation. The visualized images on the initiation process shown in Fig. 2 essentially agree with the schlieren photographs of the previous experimental work [1].

Figure 3 shows the trajectories of triple points by maximum pressure contour at each time with various ignition energies, which are varied from 100×10^6 to 338×10^6. The result of the lowest ignition energy case in Fig. 3a denotes the detonation failure, where no triple point is observed and the wave front expands spherically. In addition, the maximum pressure decays with the increase in the distance from the ignition source, due to the deceleration of the shock wave. In the case that is slightly below the minimum ignition energy of Fig. 3b, few triple points are observed near the ignition source, but the triple points disappear and the maximum pressure becomes lower in the expanding of the wave front, because of the combustion termination. The results of the subcritical regime in Figs. 3a and 3b indicate that the influence of ignition energy is observed in the propagating velocity and the shape of the blast wave. At the critical energy in Fig. 3c, although few triple points disappear near the ignition source as well as the subcritical regime in Fig. 3b, the cellular pattern is generated after the onset of the multiheaded detonation wave. The cellular pattern expands from the initiation point, where the cell width is larger than that of the surrounding. After the establishment of the fully developed detonation wave, the regularly located cellular pattern is observed. The result corresponds to the previous experimental work by Vasil'ev and Trotsyuk [7], which has reported the disappearance of triple points near the ignition source and the formation of new triple points after the detonation initiation. In the results of the supercritical regime in Figs. 3d – 3f, the cellular pattern radiates regularly out from the ignition center. These images of cellular pattern agree with the previous experimental study [13], which is an open shutter photograph in the spherical detonation propagating in open-space, after propagating through a circular tube. Meanwhile, the influence of ignition energy is observed in the cell width near the ignition core, and the cell width becomes smaller with the increase of ignition energy. The results agree with the previous experimental work by Edwards *et al*. [4], which has demonstrated that the growth rate of cells near the ignition source depends on the ignition energy, but the cell pattern on the fully developed detonation is not independent of the ignition energy, and then the cellular pattern looks regular, as observed in the critical regime of Fig. 3c.

Figure 4 shows the average propagation velocity in every time interval of 5 and the shock pressure on the X=Y line versus the distance from the ignition center for the ignition energy of (a) 137×10^6, (b) 137.5×10^6, (c) 150×10^6 and (d) 338×10^6. The

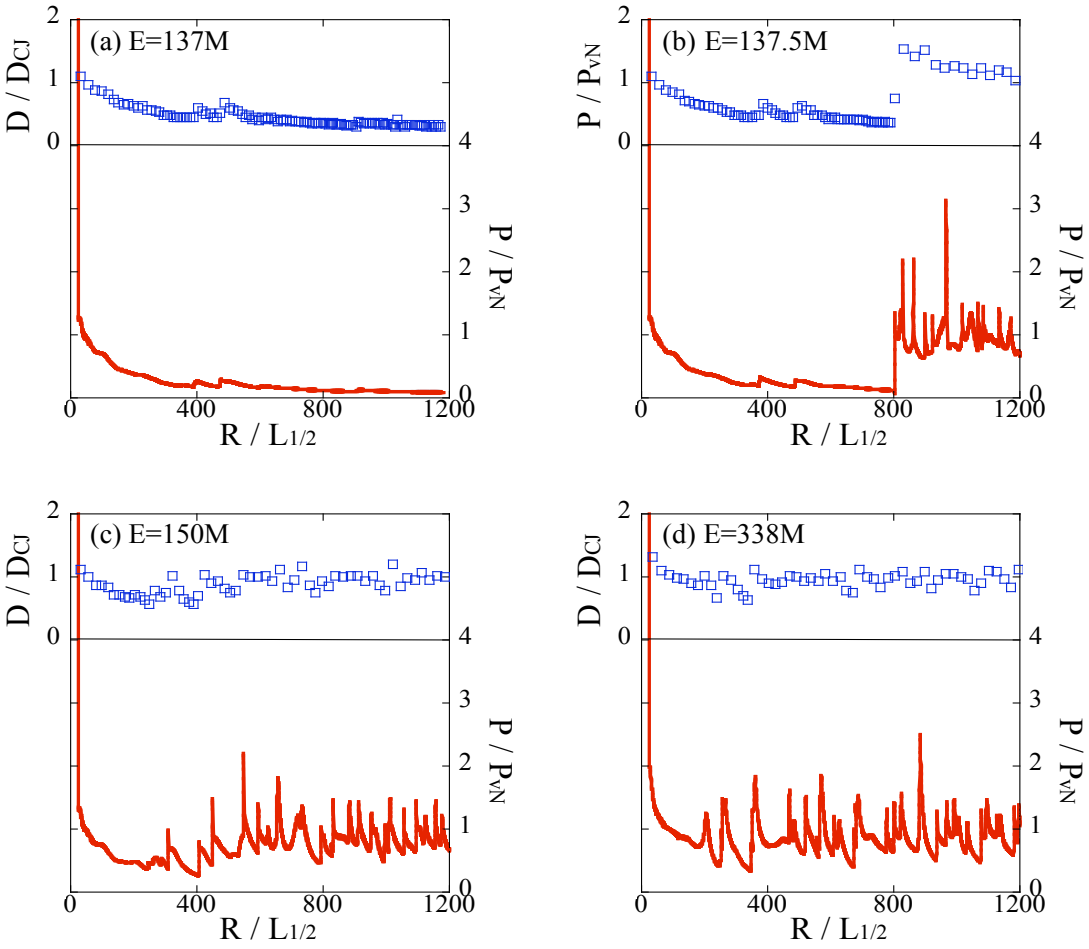

p

Fig. 4 Average propagation velocity D and shock pressure on X=Y line versus distance from ignition core for the cases of (a) 137×10^6, (b) 137.5×10^6, (c) 150×10^6 and (d) 338×10^6. (D_{CJ}=4.705, P_{vN}=20.03)

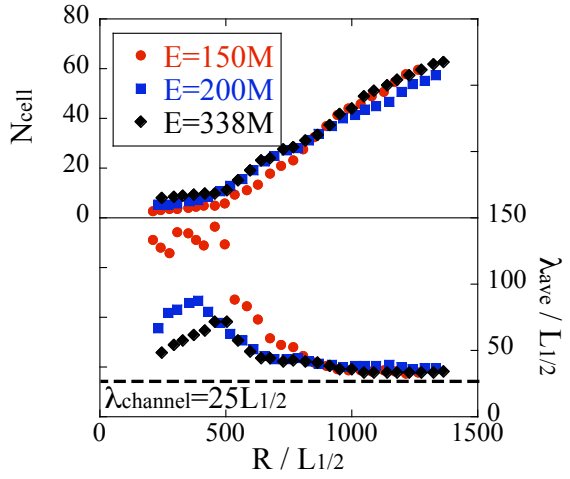

Fig. 5 Number of cells N_{cell} and average cell width λ_{ave} in the supercritical regime of Figs. 3d- 3f versus distance from ignition core. (average cell width in channel: $\lambda_{channel}=25L_{1/2}$)

results are normalized by the CJ conditions (D_{CJ}=4.71, P_{vN}=20.03). In the subcritical regime of Fig. 4a, the shock pressure keeps decaying during propagation. In the critical regime of Fig. 4b, after the pressure continue to decrease as well as the subcritical regime in Fig. 4a, the pressure drastically increases at $R=800L_{1/2}$. The pressure rise is identical to the onset of the detonation, in which the detonation bubble engulfs the leading shock wave and the shock-heated premixed gas on the X=Y line, as observed in Fig. 2b. After the detonation initiation, the average propagation velocity is almost equal to the CJ speed, and the irregular pressure jumps are observed, due to the collisions of triple points. Comparison of the results in the supercritical regime of Figs. 4c and 4d, the effect of ignition energy appears at the early stage of the detonation initiation. Although at the lower energy case of Fig. 4c, detonation is initiated after the pressure decrease near the half-CJ pressure, in the higher energy case of Fig. 4d, the blast wave directly develops into the detonation during the pressure decay in the higher energy case of Fig. 4d. Therefore, the location where the first pressure jump appears gets closer to the ignition center at the higher energy case. After the initiation, the detonation wave propagates at the CJ velocity with the irregular pressure jumps in both cases, as observed in the critical regime of Fig. 4b. The results imply that the propagation velocity and the behavior at the wave front after the establishment of fully developed detonation are independent of ignition energy.

Table 1 Specific data in Fig. 5 versus ignition energy E. λ_{max}: Maximum value of average cell width in Fig. 5, R*: Location at λ_{max}, λ_{1000}: cell width at R=1000$L_{1/2}$.

E	R*/$L_{1/2}$	$\lambda_{max}/L_{1/2}$	$\lambda_{1000}/L_{1/2}$
150M	456.4	143.4	35.6
200M	388.6	87.2	36.1
338M	504.5	72.0	34.3

Figure 5 shows cell number N_{cell} and average cell width λ_{ave} at the detonation front in the supercritical regime of Figs. 3d - 3f versus distance from the ignition center. Table 1 shows the specific data in Fig. 5, where λ_{max}, R*, and λ_{1000} are the maximum value of average cell width, the location at the maximum cell width, and the cell width at R=1000$L_{1/2}$, respectively. λ_{1000} is the data of the fully developed detonation. The cell width of the two-dimensional planar detonation propagating in sufficiently wide channel ($\lambda_{channel}$=25$L_{1/2}$) is also drawn as reference data in Fig. 5. As shown in Fig. 5, N_{cell} remains constant near the ignition source and starts to increase after R=400-500$L_{1/2}$. Meanwhile, λ_{ave} increases to the maximum value and approaches a value slightly above the reference data. R* corresponds to the location where the cells start to increase in number, and the maximum value implies the onset of the formation of new triple points. Namely, the propagation process is classified into the two stages. In the first stage, which is observed near the ignition source, the cells grow with the detonation propagation while the cells number remains unchanged. In the second stage, due to the spontaneous formation of new triple points, the cell maintains constant width, which is slightly bigger than the reference data on the channel flow, during the expanding process of the detonation. The latter stage demonstrates the previous experimental work by Vasil'ev and Trotsyuk [7], which has reported the formation of new triple points in the expanding of the wave front. The influence of ignition energy is observed in the maximum cell width λ_{max}, the width λ_{max} becomes smaller with the increase in ignition energy. Meanwhile, the average cell width in the critical regime of Fig. 3c is about 36.8$L_{1/2}$, and the results quantitatively agreed with that of the supercritical regime. Therefore, the width λ_{ave} on the fully developed detonation are independent of ignition energy, similarly to the propagation velocity and the shock pressure behaviors. In addition, the cell number N_{cell} in the supercritical regime is independent of ignition energy as well as the average cell width.

Conclusion

The initiation and propagation processes of the spherical detonation initiated by direct initiation were investigated using two-dimensional compressible Euler equations for axisymmetry with a one-step reaction model governed by Arrhenius's form with the various levels of ignition energy. Under this calculation condition, the minimum ignition energy to initiate a spherical detonation wave is 137.5x10^6, which is less than the critical energy of the one-dimensional detonation reported by the previous numerical work. The three initiation processes, which are the subcritical, critical and supercritical regimes, are observed by varying ignition energy. In the subcritical regime, the reaction front is decoupled from the blast wave generated from the high-energy core just after ignition, and detonation is not initiated. In the supercritical regime, the leading shock wave develops into the multiheaded detonation wave and the regularly located cellular patter radiates from the ignition center. The effect of ignition energy appears in the early stage of the detonation initiation. The cell width becomes smaller and the location where the first pressure jump appears gets closer to the ignition center with the increase in ignition energy. In the critical regime, the reaction front separates from the blast wave, as occurs in the subcritical regime just after ignition, but the detonation bubble generated by the local explosion behind the leading shock wave expands and develops into the multiheaded detonation wave. Although few triple points disappears near the ignition core, the cellular pattern expands from the location, where the local explosion occurs, after the detonation initiation. By changing the ignition energy, the different initiation processes are observed, but the propagation process after the establishment of the fully developed detonation is independent of ignition energy. Therefore, the multiheaded detonation propagates at the CJ velocity and the cell maintatin the constant width that is slightly greater than the cell width in channel flow, regardless of ignition energy. The numerical results qualitatively agree with the experimental study regarding the initiation process and the behaviors of the cellular structure during the propagation.

References

1) Lee, J. H. S.: INITIATION OF GASEOUS DETONATION, *Ann. Rev. Phys. Chem.*, **28**, 1977, pp. 75-104.
2) Lee. J. H., and Ramamurthi, K.: On the Concept of the Critical Size of a Detonation Kernel, *Combust. Flame*, **27**, 1976, pp. 331-340.
3) Matsui, H., and Lee, J. H. S.: The 17th Symp. (Int.) Combust., 1978, pp. 1269-1280.
4) Edwards, D. H., Hooper, G., Morgan, J. M., and Thomas, G. O.: The quasi-steady regime in critically initiated detonation waves, *J. Phys. D., Appl. Phys.*, **11**, 1978, pp. 2103-2117
5) Lee, J. H. S.: DYNAMIC PARAMETER OF GASEOUS DETONATIONS, *Ann. Rev. Fluid Mech.*, **16**, 1984, pp. 311-336.

6) Lee. J. H. S. and Higgins, A. J.: Comments on criteria for direct initiation of detonation, *Phil. Trans. R. Soc. Lond. A*, **357**, 1999, pp. 3503-3521.
7) Vasil'ev, A. A., and Trotsyuk, A. V.: Experimental Investigation and Numerical Simulation of an Expanding Multifront Detonation Wave, *Combust., Explosion, and Shock Wave*, **39**, 2003, pp. 80-90.
8) Mazaheri, K., and Lee. J. H. S.: The 16th International Colloquium on the Dynamics of Explosions and Reactive Systems, 1997, pp. 216-219.
9) Eckett, C. A., Quirk, J. J., and Shephard, J. E.: The role of unsteadiness in direct initation of gaseous detonations, *J. Fluid Mech.*, **421**, 2000, pp. 147-183.
10) Watt, S. D., and Sharpe, G. J.: Linear and nonlinear dynamics of cylindrically and spherically expanding detonation waves, *J. Fluid Mech.*, **522**, 2005, pp. 329-356.
11) Nirasawa, T., and Matsuo, A.: The 21st International Colloquium on the Dynamics of Explosions and Reactive Systems, 2007, paper 217.
12) Yee, H. C.: Upwind Scheme and Symmetric Shock Capturing Schemes, NASA TM-89464, 1987.
13) Lee. J. H. S. In: Bowen. J. R., Editor, *Dynamics of Exothermicity*, Gordon and Breech Publishers, Netherlands, 1996, pp.321-336.